2000

Modeling the Effects of Ion Association on Direct-Current Polarization of Solid Polymer Electrolytes

Changqing Lin
University of South Carolina - Columbia

Ralph E. White
University of South Carolina - Columbia, white@cec.sc.edu

Harry J. Ploehn
University of South Carolina - Columbia, ploehn@cec.sc.edu

Publication Info

Journal of the Electrochemical Society, 2000, pages 936-944.

Publisher's link: http://dx.doi.org/10.1149/1.1393295
DOI: 10.1149/1.1393295

Journal of The Electrochemical Society, **147** (3) 936-944 (2000)
S0013-4651(99)07-063-9 CCC: $7.00

Modeling the Effects of Ion Association on Direct-Current Polarization of Solid Polymer Electrolytes

Changqing Lin, Ralph E. White,* and Harry J. Ploehn[z]

Department of Chemical Engineering, University of South Carolina, Swearingen Engineering Center, Columbia, South Carolina 29208, USA

Considerable experimental evidence indicates that ion association occurs in solid polymer electrolytes. This work provides a thorough theoretical analysis of the effect of ion association on the conductivity, general current-potential behavior, and limiting current density in a solid polymer electrolyte. The model employs dilute solution theory to describe the fluxes of cations, anions, and ion pairs in a motionless continuum but neglects higher order association. The predictions of the model highlight the effects of the relative diffusion coefficients and dimensionless association constant on concentration distributions of simple ions and ion pairs, the limiting current density, and the potential drop required to drive a specified current density. If ion pairs have a diffusivity comparable to those of cations and anions, increasing ion association leads to a continuous decrease in molar conductivity and current density at constant applied potential. If the ion pairs have a diffusivity that is large compared to cations, the situation is quite different. In this case, ion association increases the limiting current density to values that may be several times that found in the case of full dissociation. Furthermore, the model predicts maxima in the molar conductivity and current density at fixed potential drop as the degree of ion association increases.

Manuscript submitted July 13, 1999; revised manuscript received November 2, 1999.

Polymer electrolytes are solid ionic conductors formed by dissolving salts in polymers containing Lewis base polar atoms. The salt typically consists of an alkali metal cation with a large anion, such as $LiCF_3SO_3$ or $LiClO_4$. The oxygen atoms in polyethers poly(ethylene oxide) (PEO) and poly(propylene oxide) (PPO), serve as Lewis bases which form complexes with the cations according to

$$(\text{–P–})_n + \text{AB} \rightarrow (\text{–P–})_n\text{A}^+ + \text{B}^- \qquad [1]$$

where (–P–) represents the polymer repeat unit and AB represents the alkali metal salt. Since Armand *et al.*[1] first proposed the use of poly(ethylene oxide) (PEO) as a solid electrolyte, much effort has been devoted to understanding ion-transport mechanisms in polymer electrolytes and to developing new materials with improved transport and mechanical properties.[2,3]

The mechanisms of ion transport in polymer electrolytes are not completely understood. Various molecular models of ion transport have been reviewed by Ratner.[2] Complementary experimental investigations[3] reveal strong interactions between the polymer host and cations. Considerable experimental evidence also suggests that strong cation-anion (A^+, B^-) interactions lead to the formation of ion pairs (AB), triplets (A_2B^+ and AB_2^-), as well as higher order clusters.

MacCallum *et al.*[3,4] and Ratner[2] have reviewed experimental studies of ion association phenomena in polymer electrolytes. Conductance measurements[3-6] and spectroscopy[2,8-13] have been used most commonly. The conductance method examines the dependence of conductivity on salt concentration, c_0. In the absence of ion association, conductivity is proportional to c_0. Association of simple ions to form ion pairs leads to measured conductivity values proportional to $\sqrt{K_d c_o}$, where K_d denotes the equilibrium constant for dissociation. MacCallum *et al.*[3,4] used this method to investigate ion association for $LiClO_4$ and $LiCF_3SO_3$ salts in PEO. Their data suggest that ion pairs and higher order clusters greatly outnumber the simple ions in PEO.

A variety of spectroscopic methods[8-13] have also been used to identify ion pairs and higher order clusters in polymer electrolytes. For example, Mitani and Adachi[8] measured the dissociation equilibrium of LiSCN in DMF/PPO using infrared spectroscopy. Absorption bands indicated the existence of simple ions, ion-pairs, and dimers [$(LiSCN)_2$], but no triplets. The dissociation constant decreased with decreasing dielectric constant in agreement with theory.[2] Kakihana *et al.*[9] employed Raman spectroscopy to investigate the dissociation equilibrium of Li and Na salts of $CF_3SO_3^-$ and ClO_4^- in PPO. Vibrational spectroscopy[10] has provided clear evidence for the existence of ion pairs in $LiBH_4$/PEO and $NaBH_4$/PEO. The work of Schantz *et al.*[11,12] indicates that the degree of dissociation would decrease with increasing temperature or polymer molecular weight. Their data do not suggest the presence of triplets, in contrast with the predictions of MacCallum *et al.*[3,4]

Although the population distributions of ions and clusters are not known precisely, the experimental evidence strongly supports the view that ion association occurs in most polymer electrolytes studied to date. We expect ion association to have a profound effect on the polymer electrolyte's transport properties. The accuracy of methods used to measure ionic diffusivity, mobility, and transport number depends on the nature of ion association in the system. Furthermore, ion association should have a significant effect on one's strategy for optimizing the performance of battery cells.[14] None of the existing models[15] for predicting battery performance accounts for ion association in polymer electrolytes.

Previous Ion Association Models

Bruce *et al.*[16,17] and Cameron *et al.*[18,19] first considered the effect of ion association on ion transport in polymer electrolytes. They assumed steady-state transport under dc polarization with no convection in the solid polymer electrolyte. For the case of complete salt dissociation, only cations carry current, and the ion concentration profiles are linear. Bruce and Vincent[16] extended this classic solution to account for finite electrode kinetics and nonideal electrolytes manifesting long-range ion-ion interactions and concentration-dependent diffusivities. Subsequent work[17-19] accounted for ion association in ideal electrolytes. Diffusion coefficients were treated as constant under the assumption of dilute solution theory, but ions were assumed to associate to form ion pairs as a distinct chemical species. Association is modeled as a homogeneous equilibrium reaction with only cations reactive at the electrodes. In this case, both cations and anions may carry current. When ion association is strong and ion pairs are more mobile than cations, ion pairs shuttle the cations across the electrolyte and the counterflow of anions carries most of the current. This rationalizes the low cation transference numbers seen in relatively conductive polymer electrolytes.[19] These models suggest that current-potential behavior can be used to quantify the extent of ion association. Subsequent experiments[20] utilized

* Electrochemical Society Fellow.
[z] E-mail: ploehn@engr.sc.edu

S0013-4651(99)07-063-9 CCC: $7.00

this suggestion. Armstrong and Wang[21] extended the model of Bruce *et al*. to systems containing divalent cations.

The previous models account for ion association but examine current-potential behavior only in the limit of small applied potential. Although the ionic and ion-pair concentration profiles are quadratic in general,[17] they become linear in the limit of small applied potential. The current-potential behavior at finite applied potential has not been discussed in the literature. In particular, the effect of ion association on limiting current density has not been explored. Scrosati[22] calculated the limiting current density in the polymer electrolyte solution using an expression[23] that is strictly valid only for strong electrolytes.

Some literature is available[24-26] which analyzes the limiting current density for microelectrodes in weak electrolyte solutions. All this work assumes microelectrodes with small area-to-volume ratios in semi-infinite electrolyte solutions with ions and ion pairs in equilibrium. Oldham[26] gave an exact theoretical treatment of the limiting current density for microelectrodes with spherical symmetry for both unsupported and fully supported electrolytes. In this analysis, all species have distinct diffusion coefficients. Previous analyses[24,25] introduced an apparent diffusion coefficient representing an average of cation and ion-pair diffusivities weighted by the degree of dissociation. Depending on the weighting approach, the apparent diffusion coefficient may be between those of cations and anions[24] or greater than both.[25]

In this work, we develop a general model for transport in polymer electrolytes which accounts for ion association. Our aim is to provide a rigorous foundation that encompasses previous models[17-19] and brings them to completion. For this reason, we continue to use dilute solution theory[27] to describe species fluxes, ignoring long-range ion-ion interactions treated by concentrated solution theory.[27] Casting the model equations in dimensionless form identifies characteristic groups that aid our interpretation of the model's predictions, especially focusing on the effect of ion association. We identify limiting-case solutions that connect this model with previous results. In addition, we explore the effects of ion association on limiting current density, current-potential behavior at arbitrary applied potential, and effective conductivity at small applied potential.

Continuum Transport Model

Assumptions.—Here we develop a simplified continuum model for transport and reaction of ionic species in polymer electrolytes. To simplify the problem, we invoke several assumptions.

1. The domains of the electrode and electrolyte phases (Fig. 1) have planar symmetry with no variations in the lateral dimensions.

2. The electrolyte phase consists of immobile, nonreactive polymer, univalent cations (A^+), univalent anions (B^-), and ion pairs (AB). No supporting salts are present. We do not consider higher order aggregates (triplets, etc.).

3. The polymer concentration is constant. The concentrations of A^+, B^-, and AB, denoted by c_+, c_-, and c_p, vary with position but not time. The total salt concentration, c_0, is a known, constant parameter.

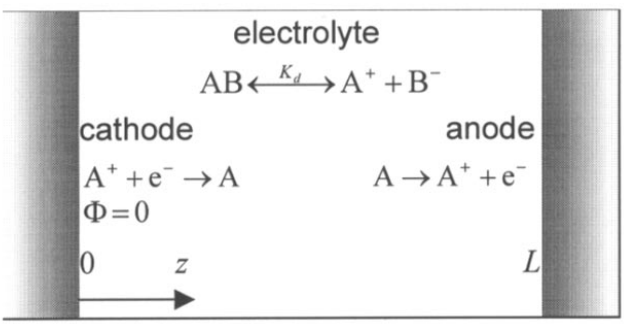

Figure 1. An electrolyte phase ($0 < z < L$) containing A^+, B^-, and AB bounded by cathode and anode phases.

4. Dilute solution theory[27] describes the transport of A^+, B^-, and AB. The species' diffusion coefficients are defined as effective binary coefficients and are constant.

5. Electroneutrality implies that at all positions

$$c_+ = c_- \qquad [2]$$

6. Equilibrium between ions and ion pairs is represented by the reaction

$$AB \overset{K_d}{\rightleftharpoons} A^+ + B^- \qquad [3]$$

where K_d denotes the dissociation constant. Consequently, the concentrations of A^+, B^-, and AB are related by

$$K_d = \frac{c_+ c_-}{c_p} = \frac{c_+^2}{c_p} \qquad [4]$$

with the second equality arising due to Eq. 2. We assume that equilibration is fast compared to all other processes. The molar production rates of A^+, B^-, and AB are related by

$$R_+ = R_- = -R_p \qquad [5]$$

based on the univalent stoichiometry implied by the reactions shown in Eq. 3.

7. Only cations are electroactive at the electrolyte-electrode interfaces. We have

$$A^+ + e^- \rightarrow A \qquad [6]$$

at the cathode located at $z = 0$, and the opposite reaction at the anode located at $z = L$. The net rate of generation of A^+ due to interfacial reactions (superscript σ) is denoted as R_+^σ.

8. Combining the reactions in Eq. 3 and 6 indicates that ion pairs may supply or take up cations consumed or generated by interfacial reactions. This implies that anions and ion pairs may be generated or consumed due to interfacial reactions. The corresponding net production rates due to interfacial reactions are related by

$$R_-^\sigma = -R_p^\sigma \qquad [7]$$

These rates are not directly related to R_+^σ, since the A^+ appearing in Eq. 6 may come from ion pairs or free cations.

The rates of interfacial reactions are fast compared to all other processes in the system. We do not treat the case of finite electrode kinetics here.

Transport equations.—The complete development of governing equations describing the transport of A^+, B^-, and AB in a polymer electrolyte is given in the Appendix. In brief, the development begins with expressions for the component mass balances, Eq. A-1, simplified in view of assumptions 1-3. Equilibrium among the various species in solution and the stoichiometry of surface reactions lead to further simplifications. Specifically, the analysis shows that the anion flux must be balanced by a counterflux of ion pairs at every location in the electrolyte. Assumption 4 introduces expressions for the fluxes in terms of concentration and potential gradients as well as the total ionic current. Finally, a mass balance on element A relates the A^+ and AB concentrations to the nominal salt concentration c_0. The development produces a first-order differential equation, Eq. A-9, with Eq. A-10, providing the integration constant. Equation A-7 can then be solved for the potential distribution.

For convenience, we cast Eq. A-7, A-9, and A-10 in dimensionless form. Defining the dimensionless variables as shown in Table I, these become

$$\frac{\partial \Phi}{\partial Z} = \frac{1}{C_+}\frac{\partial C_+}{\partial Z} + 2\Pi_A \Pi_{pa} \frac{\partial C_+}{\partial Z} \qquad [8]$$

$$2\Pi_I = \frac{\partial C_+}{\partial Z} + \Pi_{ps}\Pi_A C_+ \frac{\partial C_+}{\partial Z} \qquad [9]$$

S0013-4651(99)07-063-9 CCC: $7.00

Table I. Dimensionless variables and groups.

Variables	Physical meaning
$Z \equiv z/L$	Dimensionless position
$C_i \equiv c_i/c_0$	Dimensionless concentration of species i
$\Phi \equiv F\phi/RT$	Dimensionless potential
Groups	
$\Pi_{ps} = D_p\left(\frac{1}{D_+} + \frac{1}{D_-}\right)$	Dimensionless ion-pair diffusivity relative to "salt" diffusivity
$\Pi_{pa} = \frac{D_p}{D_-}$	Dimensionless ion-pair diffusivity relative to that of anions
$\Pi_A = \frac{c_0}{K_d}$	Dimensionless ion-pair association constant
$\Pi_I = \frac{I}{4D_+c_0F/L}$	Dimensionless current density

and

$$\int_0^1 \left(C_+ + \Pi_A C_+^2\right) dZ = 1 \qquad [10]$$

after using Eq. 4 to relate c_+ to c_p. Table I provides the definitions and physical interpretations of the dimensionless groups appearing in these equations.

General analytic solution.—After specifying the dimensionless groups as in Table I, Eq. 8 and 9 can be solved analytically for Φ and C_+. We find

$$C_+ = \frac{-1 + \sqrt{1 + 2\Pi_{ps}\Pi_A(2\Pi_I Z + A)}}{\Pi_{ps}\Pi_A} \qquad [11]$$

as long as $\Pi_{ps} \neq 0$ and $\Pi_A \neq 0$. The quantity A is an integration constant calculated using Eq. 10. For the electric potential, we obtain

$$\Phi = \ln\frac{-1 + \sqrt{1 + 2\Pi_{ps}\Pi_A(2\Pi_I Z + A)}}{-1 + \sqrt{1 + 2\Pi_{ps}\Pi_A A}} + \frac{2\Pi_{pa}}{\Pi_{ps}}\left[\sqrt{1 + 2\Pi_{ps}\Pi_A(2\Pi_I Z + A)} - \sqrt{1 + 2\Pi_{ps}\Pi_A A}\right] \qquad [12]$$

We have arbitrarily set $\Phi = 0$ at $Z = 0$. The dimensionless form of Eq. 4

$$C_p = \Pi_A C_+^2 \qquad [13]$$

provides the dimensionless ion-pair concentration C_p. We consider the limiting cases for $\Pi_{ps} \to 0$ or $\Pi_A \to 0$ later.

Both cations and anions carry current. The fraction of current carried by cations, f_+, is defined as

$$f_+ = \frac{N_+}{\sum_i z_i N_i} = \frac{-FN_+}{I} \qquad [14]$$

Substituting Eq. 6 and 7 into Eq. 14 and making the result dimensionless, we obtain

$$f_+ = \frac{1}{2\Pi_I}\left(1 + \Pi_A\Pi_{pa}C_+\right)\frac{\partial C_+}{\partial Z} \qquad [15]$$

Once A is known, f_+ may be calculated from Eq. 15 and 11.

The potential drop across the electrolyte is most conveniently expressed in terms of the cation concentrations at the cathode ($C_{+c} \equiv C_+|_{Z=0}$) and anode ($C_{+a} \equiv C_+|_{Z=L}$), both readily calculated from Eq. 11. The dimensionless potential drop across the electrolyte is

$$\Delta\Phi \equiv \Phi(1) - \Phi(0) = \ln\left(\frac{C_{+a}}{C_{+c}}\right) + 2\Pi_{pa}\Pi_A(C_{+a} - C_{+c}) \qquad [16]$$

This is related to the dimensionless applied potential ΔV through

$$\Delta V = \Delta\Phi + \Delta E \qquad [17]$$

where ΔE, given by

$$\Delta E = \ln\frac{C_{+a}}{C_{+c}} \qquad [18]$$

represents the potential developed across the cell due to concentration polarization. All potentials are made dimensionless by dividing by RT/F. Equations 16-18 combine to give

$$\Delta V = 2\ln\left(\frac{C_{+a}}{C_{+c}}\right) + 2\Pi_{pa}\Pi_A(C_{+a} - C_{+c}) \equiv \Delta V_1 + \Delta V_2 \qquad [19]$$

as the applied current required to obtain the specified ionic current I. In the following analysis, it is helpful to divide the applied potential into two parts, ΔV_1 and ΔV_2, corresponding to the two terms added in Eq. 19. The first part, ΔV_1, would be observed in the absence of ion association and accounts for ionic migration and concentration polarization. The second part, ΔV_2, occurs due to ion association and develops due to the additional ionic flux needed to maintain equilibrium among free ions and ion pairs.

Limiting current density.—An alternate solution scheme can be used to compute the limiting current density, denoted as $\Pi_{I,lim}$ in dimensionless form. At the limiting current density, C_+ becomes zero at the cathode

$$Z = 0\text{: } C_+ = 0 \qquad [20]$$

Instead of specifying the current and thus Π_I, we use Eq. 20 as the boundary condition to obtain A in Eq. 11. After substituting Eq. 11 into Eq. 10 and integrating, we can solve for $\Pi_I = \Pi_{I,lim}$.

Results and Discussion

Limiting current density.—Figure 2 illustrates the dependence of limiting current density ($\Pi_{I,lim}$) on the relative diffusivity of ion pairs (Π_{ps}) and the degree of association (Π_A). In general, if ion associa-

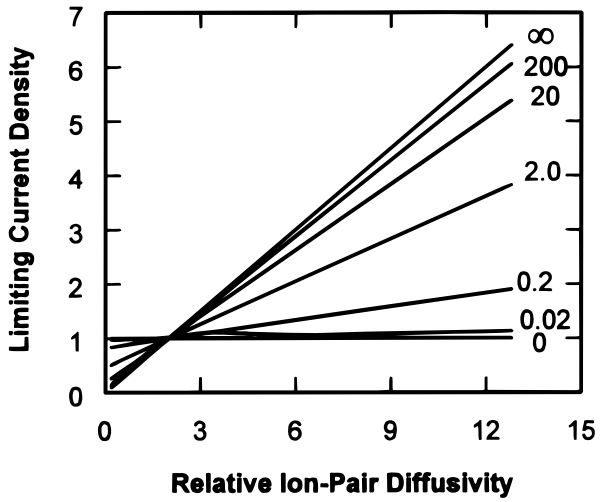

Figure 2. Dependence of limiting current density ($\Pi_{I,lim}$) on the relative diffusivity of ion pairs (Π_{ps}) and the extent of ion association (Π_A, values shown on the right).

S0013-4651(99)07-063-9 CCC: $7.00

tion occurs ($\Pi_A > 0$), the limiting current density increases with the ion-pair diffusivity. Additional insight may be gained by considering several limiting cases before further discussion of general trends.

Immobile ion pairs.—If ion pairs have no mobility ($\Pi_{ps} = 0$), Eq. 9 simplifies considerably. Integration and use of the boundary condition Eq. 20 yields

$$C_+ = 2\Pi_{I,lim}Z \quad [21]$$

Substitution into Eq. 10 and integration gives

$$4\Pi_A\Pi_{I,lim}^2 + 3\Pi_{I,lim} - 3 = 0 \quad [22]$$

For the case of complete salt dissociation ($\Pi_A = 0$), we find $\Pi_{I,lim} = 1$ and $I_{lim} = 4D_+Fc_0/L$ as expected.[22,23] Obviously, in the absence of ion pairs, $\Pi_{I,lim}$ must be independent of Π_{ps}. The corresponding curve ($\Pi_{I,lim} \equiv 1$ for $\Pi_A = 0$) can be seen in Fig. 2.

For the case of immobile ion pairs ($\Pi_{ps} = 0$) with finite ion association ($\Pi_A > 0$), Eq. 22 has the solution

$$\Pi_{I,lim} = \frac{-3 + \sqrt{9 + 48\Pi_A}}{8\Pi_A} \quad [23]$$

The limiting current density decreases with increasing association of ions as immobile ion pairs. This trend is seen in the lower left corner of Fig. 2. As $\Pi_A \to \infty$, $\Pi_{I,lim} \to 0$, showing that the electrolyte does not carry current in this limit.

Mobile ion pairs with strong association.—When ion pairs are mobile ($\Pi_{ps} > 0$)and ion association is strong ($\Pi_A >> 1$), Eq. 11 has the limiting form

$$C_+ = \sqrt{\frac{2(2\Pi_{I,lim}Z + A)}{\Pi_{ps}\Pi_A}} \quad [24]$$

To calculate the limiting current density, Eq. 20 serves as the boundary condition, yielding $A = 0$. Substituting this into Eq. 10, neglecting C_+ compared to $\Pi_A C_+^2$, and integrating lead to $\Pi_{I,lim} = 1/2\Pi_{ps}$ and $I_{lim} = \Pi_{ps}(2D_+Fc_0/L)$. This result is the uppermost curve in Fig. 2. In this case, the limiting current density depends only on the diffusivity of ion pairs relative to the average diffusivity of cations and anions.

The values of $\Pi_{I,lim} > 1$ are particularly noteworthy. In general, Π_I represents the ratio of the current density in a particular case to the limiting current density with complete dissociation. Values of $\Pi_I > 1$ indicate the passage of a higher current density than can be achieved when the ions are completely dissociated.

Mobile ion pairs with "average" diffusivity.—When $\Pi_{ps} = 2$, $D_p = 2D_+D_-/(D_+ + D_-)$ according to the definition of Π_{ps}, indicating that the ion-pair diffusivity equals the "average" salt diffusion coefficient representing a compromise between anionic and cationic diffusivities.[27] At the limiting current density, substituting $\Pi_{ps} = 2$ into Eq. 11 and using the boundary condition Eq. 20 gives

$$C_+ = \frac{-1 + \sqrt{1 + 8\Pi_A\Pi_{I,lim}Z}}{2\Pi_A} \quad [25]$$

Substituting this into Eq. 10 and integrating produce $\Pi_{I,lim} \equiv 1$. The electrolyte has a constant limiting current density equal to that in the case of complete dissociation, regardless of the extent of ion pairing. Despite the existence of ion pairs, the electrolyte behaves just as it would without ion pairing. This case is represented by the point in Fig. 2 where all the curves intersect.

General trends.—Generally (Fig. 2), the limiting current density ($\Pi_{I,lim}$) increases with ion-pair diffusivity (Π_{ps}). Ion pairs provide a parallel mechanism for transporting cations from the anode to the cathode. The counterflow of anions carries part of the required ionic current. As Π_{ps} increases, the fraction of current carried by cations decreases and ion-pair transport dominates. The effect of varying ion association (Π_A) on $\Pi_{I,lim}$ depends on whether Π_{ps} is more or less than 2. When ion pairs are less mobile than the "average" salt diffusivity ($\Pi_{ps} < 2$), $\Pi_{I,lim}$ decreases with increasing Π_A: Physically, increasing ion association effectively binds cations into less mobile ion pairs and the electrolyte cannot pass as much current. Equation 23 represents the limiting case result for immobile ion pairs.

When $\Pi_{ps} > 2$, the converse is true: increasing association produces a larger number of more mobile ion pairs and $\Pi_{I,lim}$ increases. Strong ion association leads to limiting current densities that may be several times larger than found in the case of complete ion dissociation. This implies that ion association may have favorable consequences for electrolyte performance under certain conditions. For example, Cameron *et al.*[19] claim that D_+ may be smaller than D_p due to strong interactions between cations and electronegative atoms in the polymer host. Thus, values of $\Pi_{ps} > 2$ are plausible. In such cases, the limiting current density may be increased by choosing salts which tend to form ion pairs. This conclusion must be treated cautiously, however, because the present analysis does not account for higher order clusters that may have lower mobilities.

Concentration and current fraction distributions.—Effect of ion association.—In order to understand the current-potential behavior described in the next section, it is helpful to consider in detail the effect of ion association on concentration distributions and the fraction of current carried by cations (Fig. 3). Equations 10, 11, and 12 indicate that the concentration and potential distributions are independent of the ion pair-anion diffusivity ratio, Π_{pa}. Figure 3 presents results for ion pairs that have relatively high mobility, $\Pi_{ps} = 10$, in

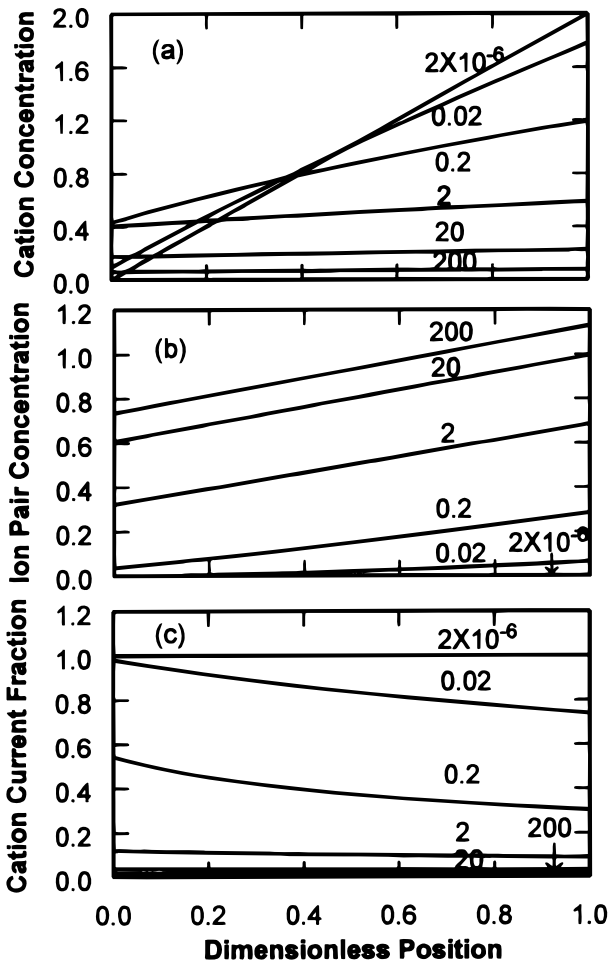

Figure 3. Effect of ion association (Π_A, values on the right) on dimensionless concentration profiles of (a) cations, (b) ion pairs, and (c) the fraction of current carried by cations for $\Pi_{ps} = 10$ and $\Pi_I = 1$. For the cation current fraction, we also have $\Pi_{pa} = 0.1$.

S0013-4651(99)07-063-9 CCC: $7.00

order to amplify the most significant trends. We also fix the current density at $\Pi_I = 1$.

In the absence of ion association ($\Pi_A = 2 \times 10^{-6}$), the cation concentration profile (Fig. 3a) is linear, falling from $C_+ = 2.0$ at the anode to zero at the cathode since $\Pi_I = 1$ is the limiting current density under these conditions. All the current is carried by cations (Fig. 3c). As ion association (Π_A) increases, the ion pair concentration increases (Fig. 3b), and the current fraction carried by cations falls (Fig. 3c) at all positions within the electrolyte, as expected. The average cation concentration decreases, as well, but the dependence of the cation concentration distribution on Π_A is more complicated. The cation concentration at the anode decreases continuously, but the cation concentration goes through a maximum before falling.

Since ion pairs have high mobility, ion association creates a facile mechanism for shuttling A^+ (within ion pairs) from the anode to the cathode and current (B^-) in the opposite direction. For $\Pi_A > 0$, the limiting current density increases (Fig. 2) to a value greater than one, because mobile ion pairs can supply additional cations. Thus, the cation concentration at the cathode initially increases with increasing Π_A. As Π_A increases above unity, the equilibrium shifts from free cations to ion pairs at all positions so that the cathode cation concentration goes through a maximum.

Figure 3c shows that the cation current fraction, and thus the cation flux, is not constant across the electrolyte, at least for intermediate values of Π_A. In fact, f_+ has its greatest value at the cathode. This indicates that cycling of ion pairs occurs, at least in part, due to association and dissociation in the electrolytic solution.

Effect of diffusivities.—When ion association is significant, the ion-pair diffusivity (relative to the salt diffusivity) has a strong influence on the cation and ion-pair distributions. In the absence of interactions with the polymer host, one might expect $\Pi_{ps} \leq 2$. However, if the polymer host binds either cations or anions, the corresponding diffusivity becomes small, so that Π_{ps} can become large. Here we consider the case of strong ion association ($\Pi_A = 200$) and a moderate current density ($\Pi_I = 0.5$). Under these conditions, most of the cations are bound in ion pairs so that the ion-pair diffusivity determines the ability of the electrolyte to carry current.

For a relatively low value of ion-pair diffusivity ($\Pi_{ps} = 1$), the value $\Pi_I = 0.5$ is just below the limiting current density (Fig. 2). Although the average ion-pair concentration (Fig. 4b) is much higher than the cation concentration (Fig. 4a), cations still carry virtually all the current (Fig. 4c). Both the cation and ion-pair concentration profiles manifest steep gradients. However, because anions carry almost none of the current, the steep ion-pair gradient is simply a consequence of equilibration with cations and anions. In this case, strong ion association clearly has an adverse impact on the ability of the electrolyte to carry current.

Doubling the ion-pair diffusivity (to $\Pi_{ps} = 2$) relaxes all the concentration gradients, since the imposed current density is only about half of the limiting value. The fraction of current carried by cations falls by almost 50%. As ion pairs become more mobile, they play a more important role in transporting A from the anode to the cathode, and the counterflux of anions carries an increasing fraction of the current. Both cation and ion-pair transport mechanisms contribute to the conduction of current in this case.

Further increases in the ion-pair diffusivity shift the balance toward the ion-pair conduction mechanism. The concentration profiles become flat due to the large relative mobility of ion pairs. The current fraction carried by cations is almost independent of position and is inversely proportional to the ion-pair diffusivity. We also find (results not shown) that f_+ increases linearly with Π_{pa}.

These trends can be predicted analytically. For strong ion association ($\Pi_A >> 1$) with $\Pi_{pa} \propto O(1)$, we have $C_+ << 1$ and $C_p \propto O(1)$. The first-term in Eq. 15 can be neglected, leaving

$$f_+ = \frac{\Pi_A \Pi_{pa}}{2\Pi_I} C_+ \frac{\partial C_+}{\partial Z} \qquad [26]$$

Also assuming that $\Pi_{ps} \geq O(1)$, Eq. 11 reduces to

$$C_+ = \sqrt{\frac{2(2\Pi_I Z + A)}{\Pi_{ps}\Pi_A}} \qquad [27]$$

Substitution into Eq. 26 gives

$$f_+ = \frac{\Pi_{pa}}{\Pi_{ps}} = \frac{D_+}{D_+ + D_-} \qquad [28]$$

The proportionality of f_+ to Π_{pa} and $1/\Pi_{ps}$ confirms the trends mentioned earlier. In addition, f_+ reduces to the definition of the transference number under these conditions. However, low cation transference number does not imply poor performance when ion association is strong and ion pairs have high mobility.

Current-potential curves.—If cations associate with the polymer host, cations should have a lower diffusivity than anions.[19] The real issue is the diffusivity of ion pairs relative to cations and anions. As suggested by Cameron *et al.*,[19] we consider ion pairs that are less mobile than anions (*i.e.*, $0 < \Pi_{pa} < 1$). We explore the effects of Π_{ps}, Π_A, and Π_{pa} on current-potential behavior.

Equal diffusivities.—For the case of $\Pi_{ps} = 2$ and $\Pi_{pa} = 1$, all species have equal diffusivities. Figure 5 shows that regardless of the state of ion association, the limiting current density reaches the expected value ($\Pi_{I,lim} = 1$) as potential drop increases. Even though all species have the same diffusivity, the potential drop required to

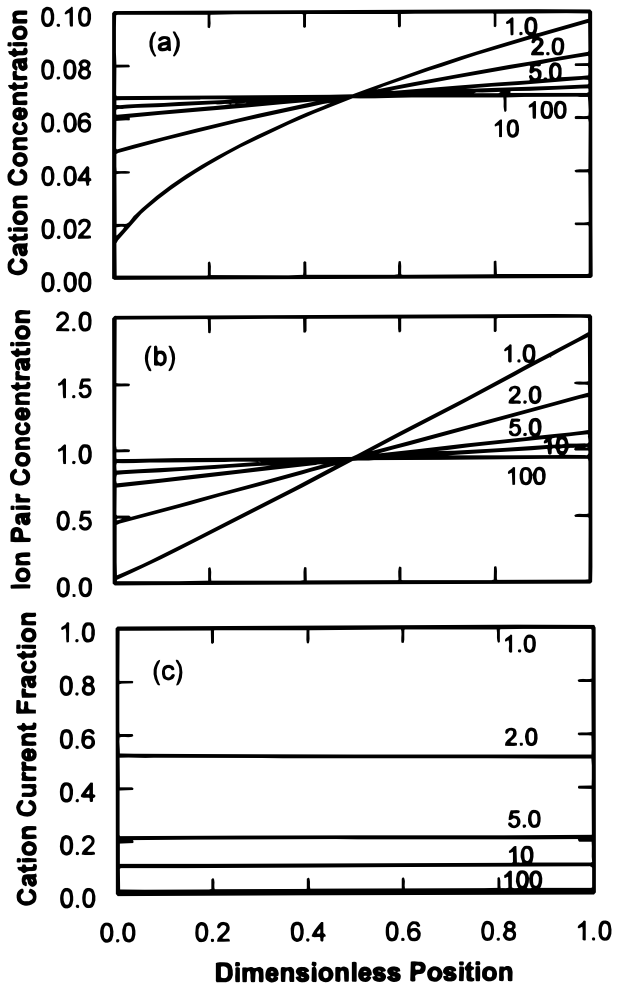

Figure 4. Effect of relative ion-pair diffusivity (Π_{ps}, values on the right) on dimensionless concentration profiles of (a) cations, (b) ion pairs, and (c) the fraction of current carried by cations for $\Pi_A = 200$ and $\Pi_I = 0.5$. For the cation current fraction, $\Pi_{pa} = 1.0$.

S0013-4651(99)07-063-9 CCC: $7.00

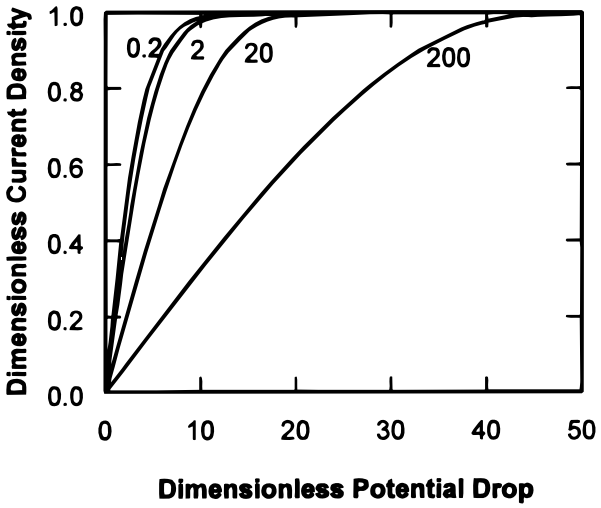

Figure 5. Effect of ion association (Π_A, values in figure) on current-potential behavior for $\Pi_{ps} = 2$ and $\Pi_{pa} = 1$.

achieve a particular current density (say, $\Pi_{I,lim} = 0.5$) increases with the degree of ion association. This can be explained in terms of the concentration profiles and the two contributions to ΔV (Fig. 6) as defined in Eq. 19. When ion association is low ($\Pi_A << 1$), cations carry most of the current (Fig. 3c), and the cation concentration gradient is steep (Fig. 3a). The cation flux from the anode to the cathode includes diffusion and migration contributions that have the same sign and are of comparable magnitude. Because the diffusive flux is large, the potential drop that drives migration remains relatively low.

As ion association increases, ion pairs shuttle cations to the cathode, and anions carry the current as they move back toward the anode. As the cation gradient relaxes with increasing Π_A (Fig. 3a), the corresponding contribution to the potential drop, ΔV_1, decreases (Fig. 6). The anion concentration and gradient also decrease (Fig. 3a, $C_- = C_+$), but the anion flux must be equal and opposite to that of ion pairs according to Eq. A-5. The potential drop thus increases to drive the migration of anions from the cathode to the anode. Figure 6 shows the contribution to the potential drop, ΔV_2, associated with this mechanism.

Figure 5 also shows that at constant applied potential, the current density decreases as ion association increases. This result is in accord with our intuition, at least when all species have equal diffusivities.

Highly mobile ion pairs.—For highly mobile ion pairs ($\Pi_{ps} = 10$), the current-potential behavior is more complex (Fig. 7). The limiting current density increases with ion association as seen earlier in Fig. 2. The potential drop required to obtain a given current density (say, $\Pi_I = 0.5$) goes through a minimum with increasing values of Π_A. Likewise, at constant applied potential, the resulting current density displays a maximum. This behavior can be explained by the mechanisms introduced earlier with allowance for the differing diffusivities of the species.

For $\Pi_{ps} = 10$ and $\Pi_{pa} = 0.1$, anions are ten times more mobile than ion pairs, and ion pairs are 9.9 times more mobile than cations ($\Pi_{ps} = \Pi_{pa} + D_p/D_+$) according to the definitions of dimensionless groups in Table I). As the equilibrium shifts toward ion pairs with increasing Π_A, the cation gradient, flux, and potential driving force ΔV_1 (Fig. 8b) all decrease. The more mobile ion pairs do not require as steep a concentration gradient to transport cations across the electrolyte. The anions, being 99 times more mobile than cations, require only a moderate increase in potential drop to generate a sufficient flux back toward the anode (contribution ΔV_2, Fig. 8b). The total potential drop at fixed current density thus goes through a minimum as ion association increases (Fig. 8a). Alternately, at fixed potential drop, the ion pair/anion shuttle provides a parallel mechanism that contributes to the total current density as Π_A increases, at least initially. At large Π_A, however, anions become scarce and the current density falls off.

With increasing Π_{pa}, anions become less mobile relative to ion pairs. As ion association (Π_A) increases in this case, the potential drop must increase more steeply to drive the required anion flux. This shifts the minimum in the total potential drop (Fig. 8a) to lower values of Π_A as Π_{pa} increases.

Electrolyte conductivity.—The conductivity of a polymer electrolyte can be readily measured and used to indicate the occurrence of ion association. An effective conductivity, σ, has been defined[17] as the ratio of current density to potential drop [$I/(\Delta V/L)$] in the limit of small applied potential. Dividing by the salt concentration and making current and potential drop dimensionless yields

$$\Lambda \equiv \frac{\overline{\Lambda}}{4D_+F^2/RT} = \frac{\Pi_I}{\Delta V} \qquad [29]$$

as the dimensionless, effective molar conductivity ($\overline{\Lambda}$ is the dimensional counterpart). Figures 5 and 7 show linear current-potential behavior for Π_I less than about 0.1, indicating that Λ is independent of applied potential when the latter is small.

Figure 9 shows the dependence of Λ on Π_A for various values of Π_{ps} and Π_{pa}. If we assume a constant value of the dissociation con-

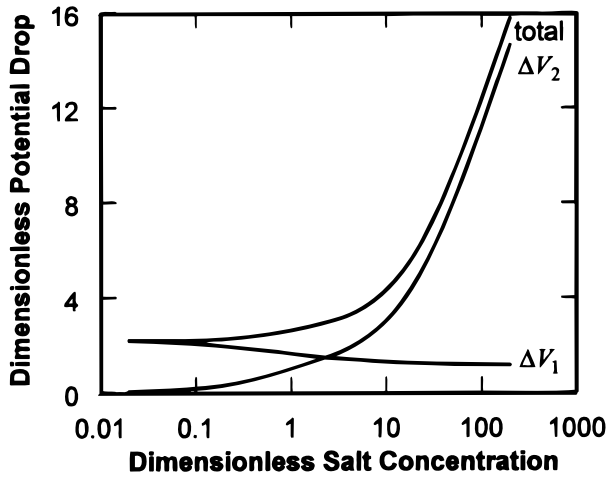

Figure 6. Effect of ion association on potential drop for $\Pi_{ps} = 2$, $\Pi_I = 0.5$, and $\Pi_{pa} = 1$.

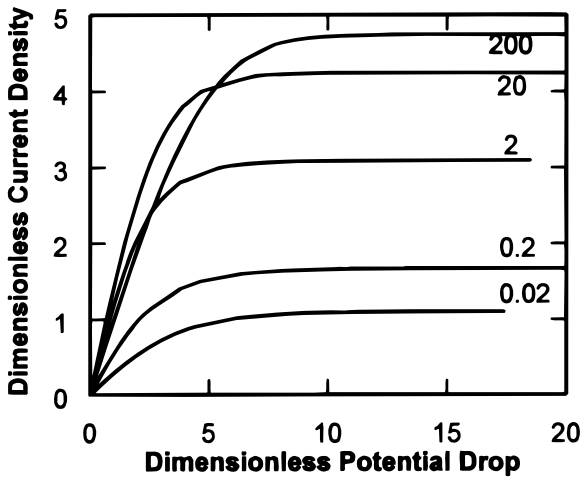

Figure 7. Effect of ion association (Π_A, values in figure) on current-potential behavior for $\Pi_{ps} = 10$ and $\Pi_{pa} = 0.1$.

S0013-4651(99)07-063-9 CCC: $7.00

stant K_d, then $\Pi_A \equiv c_0/K_d$ can be viewed as a dimensionless salt concentration. In the limit $\Pi_A << 1$ (dilute salt or large dissociation constant), Λ reaches the constant, limiting value of 0.25 that we expect for full dissociation (Eq. 29 with $\bar{\Lambda} = D_+F^2/RT$). As Π_A increases, Λ manifests a distinct maximum as long as $\Pi_{ps} > 2$. The maximal value of Λ increases with increasing Π_{ps} (Fig. 9a) and decreasing Π_{pa} (Fig. 9b). As Π_A becomes large, Λ falls toward zero independent of Π_{ps} and Π_{pa}.

These results can be easily rationalized. When $\Pi_{ps} = 2$ and $\Pi_{pa} = 1$, all species have the same diffusivity. Increasing c_0 (or decreasing K_d) leads to the formation of more ion pairs than simple ions. The conductivity, on a molar basis, thus decreases continuously. When $\Pi_{ps} > 2$, the molar conductivity initially increases with Π_A due to the formation of ion pairs that are more mobile than simple ions. The parallel mechanism involving ion pairs enables the passage of a greater current at the same applied potential. This also explains the increase in the conductivity maximum with Π_{ps} (Fig. 9a). Further increase of Π_A ultimately decreases the ability of anions to carry the current. The anion concentration decreases, and the applied potential must increase to maintain a given current density (as discussed earlier with regard to Fig. 7 and 8), leading to the decrease in Λ. As anions become less mobile relative to ion pairs (increasing Π_{pa}), the applied potential must increase in order to maintain a specified current density. For this reason, the molar conductivity decreases as Π_{pa} increases (Fig. 9b).

Figure 9b also shows experimental data[4] for the dimensionless molar conductivities of $LiClO_4$ and $LiCF_3SO_3$ dissolved in end-capped PEO. To make the conductivity data dimensionless, we assumed a value of $D_+ = 2 \times 10^{-12}$ m^2/s, so that the vertical position of the data in Fig. 9b is completely arbitrary. The dimensionless salt concentrations are expressed as the product of the experimental molal concentrations and association constants (in molal units) estimated by MacCallum *et al.*[4] from their conductivity data. Thus, the horizontal position of the data in Fig. 9b has been determined independently. This comparison supports the view[4] that the steep decrease in molar conductivity can be attributed to the formation of ion pairs and the depletion of charge-carrying simple ions at dimensionless salt concentrations well above unity. The upturn in the Λ data at higher Π_A, not seen in the model predictions, may be due to the formation of charged triplets and higher order clusters, resulting in a net increase in charge carriers. Alternately, the increase may be related to long-range ion-ion interactions (leading to concentration-dependent diffusivities) or other effects not treated in the model.

Conclusions

Our thorough theoretical analysis of the effect of ion association on transport in a solid polymer electrolyte reveals interesting behavior that had not been fully elucidated by previous models. At relatively low applied potential and current density, the model predicts a maximum in the molar conductivity. Increasing ion association generates ion pairs that can shuttle cations from the anode to the cathode with the current carried by the anion counterflux. As long as ion pairs have relatively high mobility, this increases the current density at a given applied potential as well as the molar conductivity. However, a further increase in association reduces the availability of anions; to achieve a given current density, the applied potential must increase significantly so that the molar conductivity ultimately decreases.

The same trends are evident at arbitrary values of the current density. If ion pairs have a diffusivity comparable to those of cations and

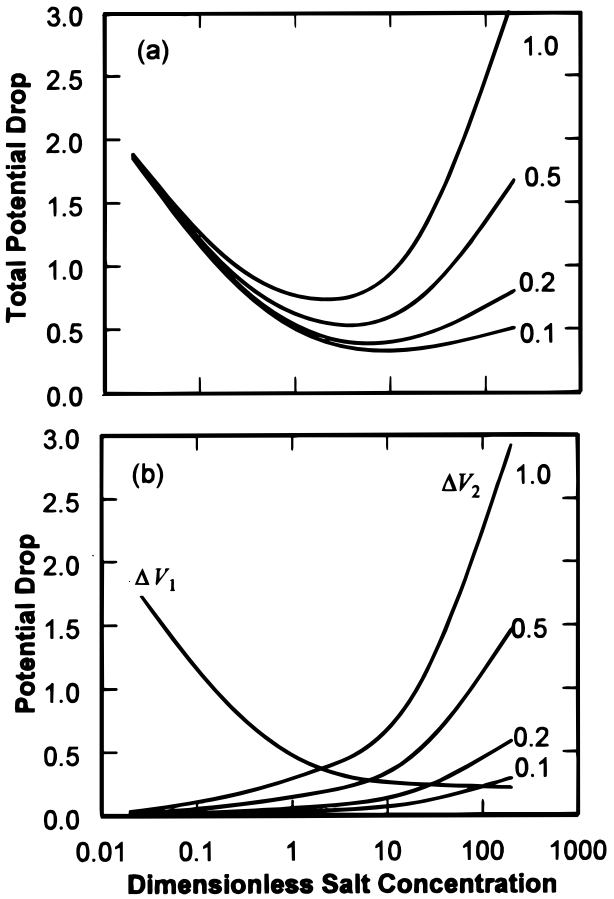

Figure 8. Effect of ion association on electrolyte potential drop for $\Pi_{ps} = 10$, $\Pi_I = 0.5$, and various values of Π_{pa} (right side of each): (a) total potential drop, ΔV and (b) contributions of ΔV_1 and ΔV_2 as defined by Eq. 19.

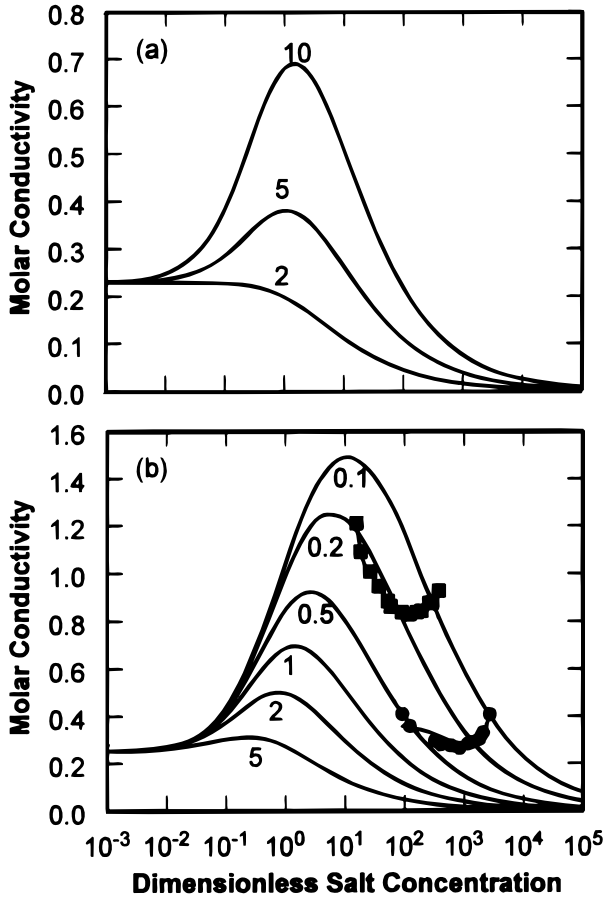

Figure 9. Dependence of dimensionless molar conductivity on dimensionless salt concentration (Π_A) for various values of Π_{ps} and Π_{pa}: (a) varying values of Π_{ps} with $\Pi_{pa} = 1$ and (b) varying values of Π_{pa} with $\Pi_{ps} = 10$. Symbols denote experimental data for (■) $LiClO_4$ and (●) $LiCF_3SO_3$ dissolved in end-capped PEO.[4]

S0013-4651(99)07-063-9 CCC: $7.00

anions, then ion association increases the potential drop required to drive a given current density or decreases the current density that can be obtained at a given potential drop.

On the other hand, ion association may offer an opportunity for enhanced performance if ion pairs have a diffusivity that is large compared to cations. The limiting current density increases with the degree of ion association in this case and may be several times greater than the limiting current density found in the full dissociation case. At a fixed potential drop, the current density goes through a maximum as ion association increases.

These results suggest a number of strategies for improving the performance of solid polymer electrolytes. If ion association occurs, current density can be maximized if the ion pair diffusivity is large compared to cations and small compared to anions. In this situation, promoting ion association can increase conductivity and current density. However, we expect a point of diminishing return due to the formation of higher order clusters with lower diffusivity.

For any salt/electrolyte system of interest, one should first try to quantify the extent of ion association. No single experiment, analyzed in conjunction with the present model, can do this. Assuming that we know the added salt concentration c_0 and can measure the current density I, the model involves three dimensionless groups (Π_{ps}, Π_{pa}, Π_A) dependent on four experimental parameters (D_+, D_-, D_p, K_d). Clearly, additional information is needed.

If we have an independent value of D_+, a measurement of the limiting current density I_{lim} gives a rapid indication of ion association. Recall that $\Pi_{I,lim} \propto I_{lim}/D_+$. If $\Pi_{I,lim} > 1$, Fig. 2 indicates that ions associate into ion pairs with relatively high diffusivity; the converse is true for $\Pi_{I,lim} < 1$. However, this quick test cannot distinguish between high levels of association into ion pairs with moderate mobility *vs*. low levels of association into pairs with very high mobility. If $\Pi_{I,lim} = 1$, we cannot tell if ion association occurs, but it does not matter since the ion-pair diffusivity cannot differ from the average salt diffusivity in this case.

A more quantitative analysis requires additional independent information. For example, it would be helpful to have measured values for both D_+ and D_-. In this situation, measurements of $\Pi_{I,lim}$ and Λ (corresponding to measurements of I at the limits of high and low applied potential) can be used to determine values of D_p and K_d. In graphical terms, we would use the measured values of $\Pi_{I,lim}$ and Λ with Fig. 2 and 9b to determine Π_A and Π_{ps}. The model equations could be solved directly for the two unknowns. It may be possible to obtain both D_+ and D_- using some combination of pulsed-field gradient nuclear magnetic resonance (NMR),[13,29-31] the Hittorf method,[19] or other techniques.[32] One must be cautious to ensure that ion association does not confound the interpretation of the data from these techniques. Alternately, it may be possible to use ac impedance experiments to yield information that complements dc experiments. We are currently developing a model that accounts for the effect of ion association on ac impedance spectra.

Acknowledgments

We acknowledge the financial support of this work by the U.S. Army Research Office under grant no. DAAH04-96-1-0422.

The University of South Carolina assisted in meeting the publication costs of this article.

Appendix

Transport Equations

Based on assumptions 1-3, the component mass balances can be written as

$$0 = -\frac{\partial N_i}{\partial z} + R_i \qquad [A\text{-}1]$$

with $i = +, -$, and p corresponding to A^+, B^-, and AB, respectively. Using Eq. 5, the anion and ion pair mass balances can be combined to give

$$\frac{\partial}{\partial z}(N_p + N_-) = 0 \qquad [A\text{-}2]$$

The component jump mass balances[28] at the cathode reduce to

$$z = 0\text{: } N_i = R_i^{\sigma} \qquad [A\text{-}3]$$

for $i = +, -$, and p. As a consequence of Eq. 7, we have

$$z = 0\text{: } N_p + N_- = 0 \qquad [A\text{-}4]$$

Integration of Eq. A-2 using Eq. A-4 as the boundary condition gives

$$N_p + N_- = 0 \qquad [A\text{-}5]$$

everywhere. Thus the anion flux must be balanced by a counterflux of ion pairs at every location in the electrolyte.

In addition to gradient diffusion, the electric potential field ϕ forces migration of charged components A^+ and $B-$. Based on assumption 4, dilute solution theory provides the molar flux expressions

$$N_i = -D_i\frac{\partial c_i}{\partial z} - \frac{D_i z_i F c_i}{RT}\frac{\partial \phi}{\partial z} \qquad [A\text{-}6]$$

for $i = +, -$, and p. The ion-pair valence is zero. Using Eq. 2, 4, and A-6, Eq. A-5 becomes

$$\frac{Fc_+}{RT}\frac{\partial \phi}{\partial z} = \frac{\partial c_+}{\partial z} + \frac{D_p}{D_-}\frac{\partial (c_+^2/K_d)}{\partial z} \qquad [A\text{-}7]$$

The ionic current density in the polymer electrolyte depends on the fluxes through

$$I = -\sum_i z_i N_i = -F(N_+ - N_-) = -F(N_+ + N_p) \qquad [A\text{-}8]$$

with the second equality employing Eq. A-5. For the case of complete dissociation with $N_- = N_p = 0$, the ionic current flows in the same direction as cations. Substituting fluxes from Eq. A-6, using Eq. 4, and eliminating the potential gradient with Eq. A-7, we find

$$\frac{I}{F} = 2D_+\frac{\partial c_+}{\partial z} + D_p\left(1 + \frac{D_+}{D_-}\right)\frac{\partial (c_+^2/K_d)}{\partial z} \qquad [A\text{-}9]$$

For a given value of the current I, this first-order equation can be solved analytically to determine the cation concentration distribution.

We require one additional constraint to determine the integration constant. A mass balance on A

$$\int_0^L (c_+ + c_p)dz = c_0 L \qquad [A\text{-}10]$$

relates the cation and ion-pair concentration profiles to the nominal salt concentration c_0. Equation 4 can be used to express c_p in terms of c_+.

List of Symbols

c_0	salt concentration, mol/cm^3
c_i	concentration of species i, mol/cm^3
C_i	dimensionless concentration of species i, $C_i \equiv c_i/c_0$
D_i	diffusion coefficient of species i, cm^2/s
ΔE	dimensionless potential difference across the electrolyte due to concentration polarization
F	Faraday's constant, 96,487 C/mol
f_i	fraction of current carried by species i
I	current density, A/cm^2
K_d	equilibrium constant for salt dissociation, mol/cm^3
L	thickness of the electrolyte phase, cm
N_i	flux of species i, mol/cm^2 s
R	gas constant, J/mol K
R_i	rate of generation of species i via homogeneous reactions, mol/cm^2 s
ΔV	total dimensionless potential difference across the electrolyte
ΔV_i	dimensionless potential differences defined in Eq. 19
z	position in the electrolyte relative to the cathode, cm
z_i	valence of species i
Z	dimensionless position, $Z \equiv z/L$

Greek

Λ	dimensionless effective molar conductivity
$\overline{\Lambda}$	dimensional counterpart of , S cm^2/mol
ϕ	electric potential, V
Φ	dimensionless electric potential, $\Phi \equiv F\phi/RT$
$\Delta\Phi$	dimensionless potential difference across the electrolyte defined as $\Delta V - \Delta E$
Π_i	dimensionless groups as defined in Table I
σ	effective conductivity, S/cm

S0013-4651(99)07-063-9 CCC: $7.00

Subscripts

+	cations
−	anions
a	at the anode surface
c	at the cathode surface
lim	at the limiting current density
p	ion pairs

Superscripts

σ	at an eletrode/electrolyte interface

References

1. M. B. Armand, J. M. Chabagno, and M. J. Duclot, in *Fast Ion Transport in Solids*, P. Vashista, J. N. Mundy, and G. K. Shenoy, Editors, p. 131, Elsevier, North-Holland, New York (1979).
2. M. A. Ratner, in *Polymer Electrolyte Reviews*, J. R. MacCallum and C. A. Vincent, Editors, p. 173, Elsevier Applied Science, London (1987).
3. J. R. MacCallum and C. A. Vincent, in *Polymer Electrolyte Reviews*, J. R. MacCallum and C. A. Vincent, Editors, p. 23, Elsevier Applied Science, London (1987).
4. J. R. MacCallum, A. S. Tomlin, and C. A. Vincent, *Euro. Polym. J.*, **22**, 787 (1986).
5. I. Albinsson, B. E. Mellander, and J. R. Stevens, *J. Chem. Phys.*, **96**, 681 (1992).
6. I. Albinsson, B. E. Mellander, and J. R. Stevens, *Solid State Ionics*, **60**, 63 (1993).
7. A. Killis, J. Le Nest, A. Gandini, and H. Cheradame, *Macromolecules*, **17**, 63 (1984).
8. K. Mitani and K. Adachi, *J. Polym. Sci. B: Polym. Phys.*, **33**, 937 (1995).
9. M. Kakihana, S. Schantz, and L. M. Torell, *J. Chem. Phys.*, **92**, 6271 (1990).
10. R. Dupon, B. L. Papke, M. A. Ratner, D. H. Whitmore, and D. F. Shriver, *J. Am. Chem. Soc.*, **104**, 6247 (1982).
11. S. Schantz, *J. Chem. Phys.*, **94**, 6296 (1991).
12. S. Schantz, L. M. Torell, and J. R. Stevens, *J. Chem. Phys.*, **94**, 6862 (1991).
13. A. Ferry, G. Orädd, and P. Jacobsson, *J. Chem. Phys.*, **108**, 7426 (1998).
14. P. G. Bruce, *Synth. Met.*, **45**, 267 (1991).
15. M. Doyle, T. F. Fuller, and J. Newman, *J. Electrochem. Soc.*, **140**, 1526 (1993).
16. P. G. Bruce and C. A. Vincent, *J. Electroanal. Chem.*, **225**, 1 (1987).
17. P. G. Bruce, M. T. Hardgrave, and C. A. Vincent, *J. Electroanal. Chem.*, **271**, 27 (1989).
18. G. G. Cameron, J. L. Harvie, and M. D. Ingram, *Solid State Ionics*, **34**, 65 (1989).
19. G. G. Cameron, M. D. Ingram, and J. L. Harvie, *Faraday Discuss. Chem. Soc.*, **88**, 55 (1989).
20. P. G. Bruce and C. A. Vincent, *Solid State Ionics*, **40/41**, 607 (1990).
21. R. D. Armstrong and H. Wang, *Electrochim. Acta*, **39**, 1 (1994).
22. B. Scrosati, in *Polymer Electrolyte Reviews*, J. R. MacCallum and C. A. Vincent, Editors, Elsevier Applied Science, London (1987).
23. R. B. Bird, W. E. Stewart, and E. N. Lightfoot, *Transport Phenomena*, John Wiley & Sons, New York (1960).
24. A. Jaworski, Z. Stojek, and J. G. Osteryoung, *Anal. Chem.*, **67**, 3349 (1995).
25. Y. Xie, T. Z. Liu, and J. G. Osteryoung, *Anal. Chem.*, **68**, 4124 (1996).
26. K. B. Oldham, *Anal. Chem.*, **68**, 4173 (1996).
27. J. Newman, *Electrochemical Systems*, Prentice-Hall, Englewood Cliffs, NJ (1991).
28. J. C. Slattery, *Advanced Transport Phenomena*, Oxford University, Oxford, U.K. (1999).
29. C. A. Vincent, *Prog. Solid State Chem.*, **17**, 145 (1987).
30. N. Boden, S. A. Leng, and I. M. Ward, *Solid State Ionics*, **45**, 261 (1991).
31. I. M. Ward, N. Boden, J. Cruickshank, and S. A. Leng, *Electrochim. Acta*, **40**, 2071 (1995).
32. P. G. Bruce and C. A. Vincent, *Faraday Discuss. Chem. Soc.*, **88**, 43 (1989).